Laboratori Nazionali di Frascati

LNF-61/17 (4. 3. 61)

C. Infante, F. Pandarese: THE TUNNEL DIODE AS A THRESHOLD DEVICE: THEORY AND APPLICATION

Laboratori Nazionali di Frascati del C.N.E.N.
Servizio Documentazione

Nota interna: n° 72
4 Marzo 1961

C. Infante and F. Pandarese: THE TUNNEL DIODE AS A THRESHOLD DEVICE: THEORY AND APPLICATION.

Summary

Due to the interesting properties of the tunnel diode, the device is extensively studied as regards its circuit behaviour. An empirical formula, approximating the diode's V-I characteristic, has been obtained. This allows calculations of rise time, delay time jitter to be carried out in certain instances; theoretical predictions based on this approximation are in good agreement with experimental results. Stability considerations and curve-plotting circuits are also studied. A high-speed discriminator - coincidence circuit using transistors and tunnel diodes is presented.

1 - Introduction

Tunnel diodes or Esaki diodes[1] are finding increasingly large applications as high - frequency devices[2-5]: this is due to the intrinsically good high frequency properties of the device coupled with other desirable properties such as small size, low power consumption, stability of characteristics with respect to temperature, commercial availability and, last but not least, low cost with respect to transistors having gain-band-width products of the same order of magnitude. The device is thus extremely promising and is being extensively studied as regards its application in computer technology[6].

The above reasons have prompted the Authors to study the device with the intent of applying it in the field of high speed electronics in the nuclear field.

2 - The V-I characteristic and its approximation.

One of the most striking features of the tunnel diode (TD) is the peculiar shape of its V-I characteristic (fig.1)

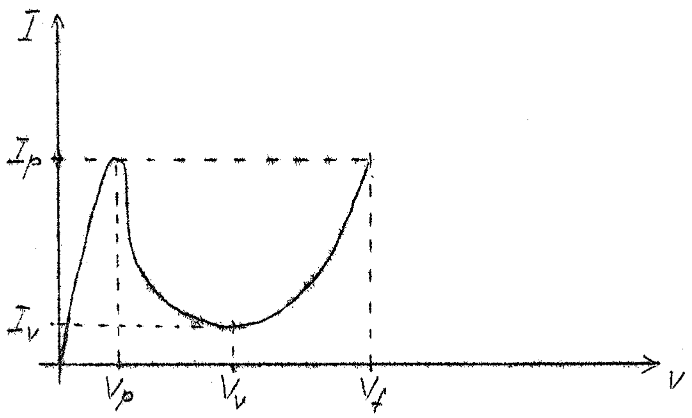

FIG. 1

small signal theory approximates the characteristic with a constant (differential) resistance whose magnitude is positive or negative according to the bias point chosen. This approach fails of course when dealing with large signals (i.e. switching circuitry). Although piece-wise linear approximation has been attempted with success(7-8), a higher order approximation has been studied with the purpose of not introducing discontinuities of the differential conductance function.

Under the assumptions

a) that the approximating function be continuous with its first order derivatives over the range of interest (0 to v_f)

b) that the functionshould be of order not higher than 2 (i.e. two parabolas joined at some intermediate point v_x) the following approximation has been derived.

$$(1) \qquad i = I_p \left[1 - \left(\frac{v}{v_p} - 1\right)^2\right] \qquad \text{for} \quad 0 \leq v \leq v_x$$

$$(2) \qquad i = K(v - v_v)^2 + I_v \qquad \text{for} \quad v_x < v \leq v_f$$

where $K = \dfrac{A I_p - I_v}{(v_x - v_v)^2}$ $\qquad v_x = v_p \dfrac{\left(\frac{v_v}{v_p} - \frac{I_v}{I_p}\right)}{\left(\frac{v_v}{v_p} - 1\right)}$

$$A = 1 - \frac{\left(1 - \frac{I_v}{I_p}\right)^2}{\left(1 - \frac{v_v}{v_p}\right)^2}$$

No justification of the formula on the basis of solid state theory will be attempted; the closeness of fit is shown by the accompanying figures (2 and 3) in which measured points of commercial diodes are compared with theoretical predictions based on equations (1) and (2) above. Fit is quite good in the low voltage region, fairly good in the negative resistance region and very poor in the high voltage region where the exponential increase of current due to minority carrier injection is much faster than the parabolic increase provided by (2).

FIGURE 2

FIT FOR PHILCO T1975

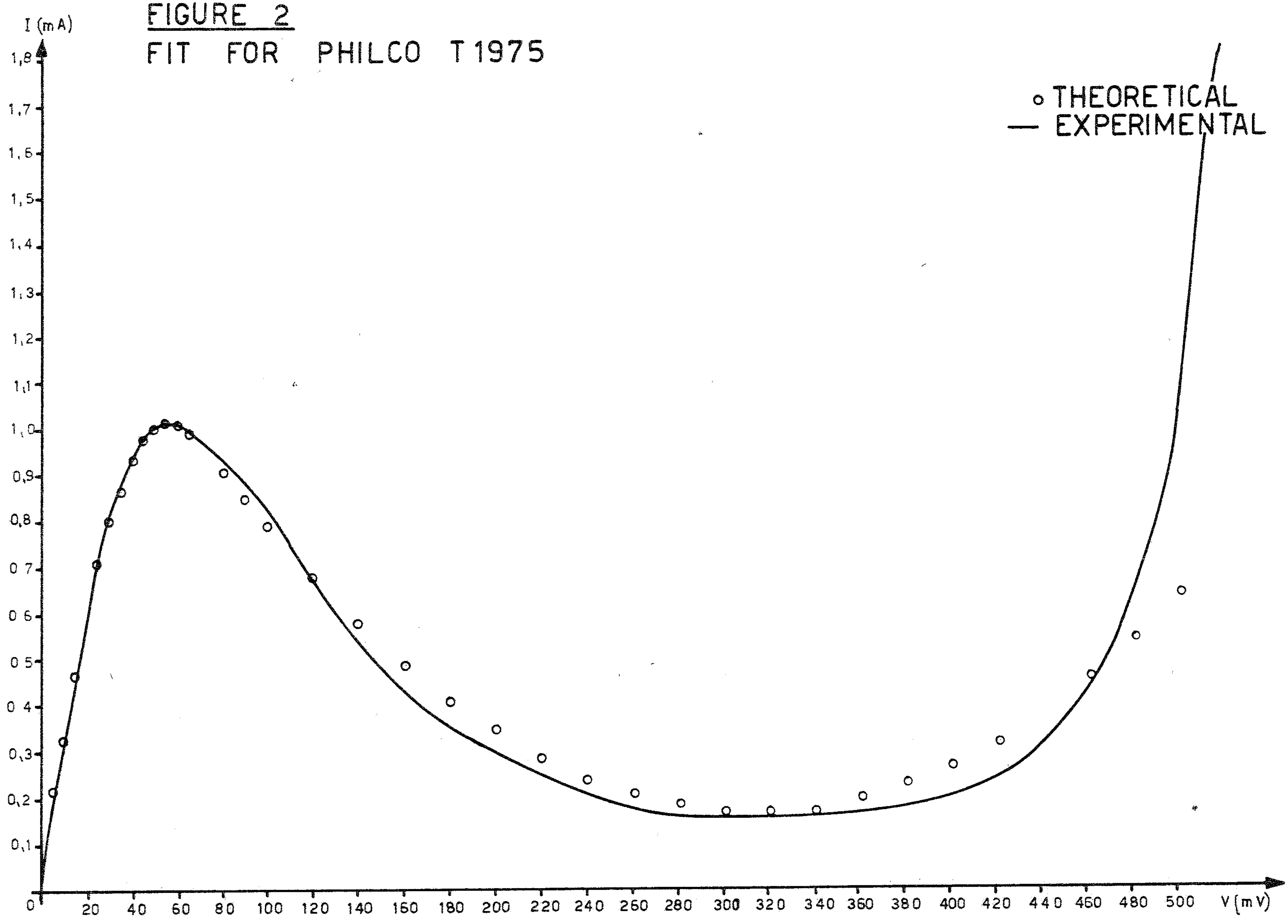

FIGURE 3

FIT FOR HOFFMAN HT 16

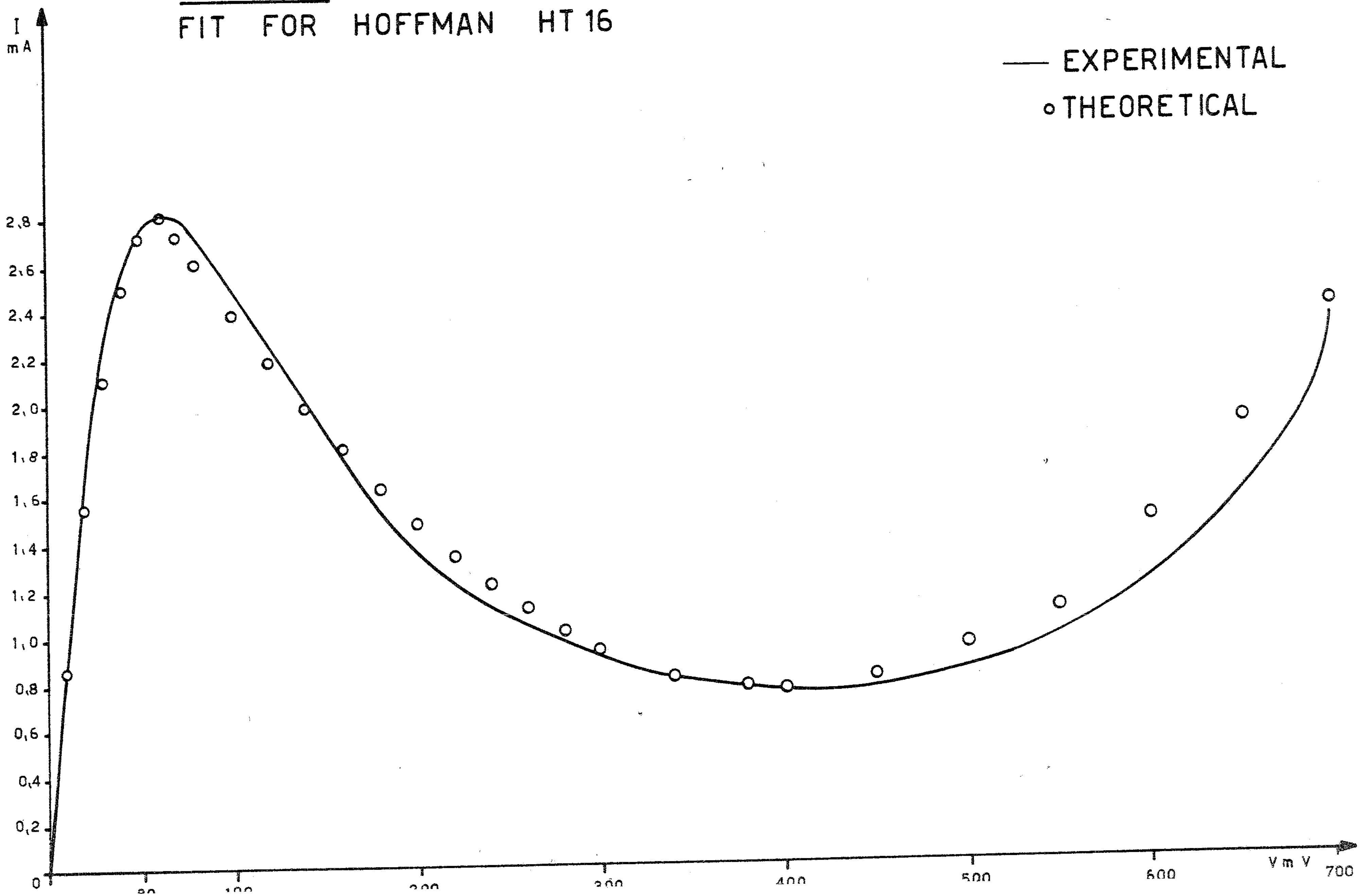

It may be interesting to note that the absolute value of the differential negative resistance has its minimum in v_x, its value being

(3) $$\left| r_{neg} \right|_{min} = \left[\frac{1}{\frac{di}{dv}} \right]_{v=v_x} = \frac{v_p^2}{2 I_p} \frac{1}{v_x - v_p}$$

Both equations (1) and (2) may be written as

(4) $$i = f(v) = k_1 (v - v_0)^2 + k_2$$

with appropriate parameter substitution.

3 - Response to a current step waveform.

Neglecting lead inductance, the TD can be thought of as a non-linear element defined by its static V-I characteristic shunted by a capacitance C(9).

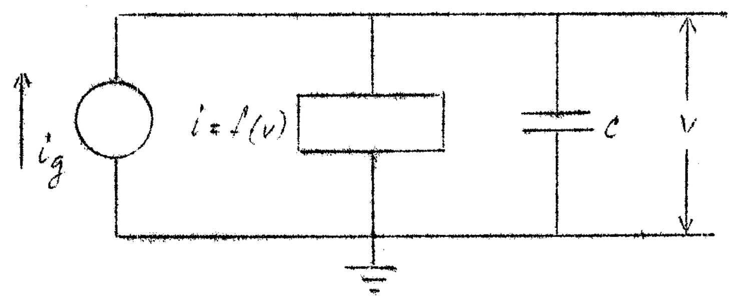

FIG. 4

Form the circuit equation, the time t necessary for the voltage V to go from 0 to a value v is given by

$$t = c \int_0^v \frac{dV}{I_g - f(V)} + K$$

where K is an integration constant that depends on the initial conditions. Substituting (I) and (2) one finds that switching time (to go from 0 to v_f) is given by

(5) $$\tau = \tau_{s1} + \tau_{s2}$$

where

$$\tau_{S1} = \frac{-v_p^2 C}{I_p C_1} tg^{-1}\left(-\frac{v_p}{C_1}\right) + \frac{v_p^2 C}{I_p C_1} tg^{-1}\left(\frac{v_x - v_p}{C_1}\right)$$

$$C_1 = v_p \sqrt{\frac{I_g}{I_p} - 1}$$

is the time to go from 0 to v_x and

$$(5') \quad \tau_{S2} = \frac{C(v_x - v_v)}{\sqrt{(I_p - I_v)(AI_p - I_v)}} \left[tgh^{-1}\left(\frac{v_f - v_v}{C_2}\right) - tgh^{-1}\left(\frac{v_x - v_v}{C_2}\right) \right]$$

is the time to go from v_x to v_f

$$C_2 = \sqrt{\frac{I_p - I_v}{AI_p - I_v}} \, (v_x - v_v)$$

examination of equations (5) and (5') shows that the predominant term is τ_{S1}, which depend strongly on I_g the input current - step amplitude. Equations (5') are in good agreement with experimental results, a plot of τ_{S1} versus I_g yielding the familiar regenerative circuit delay curve(10).

4 - Response to a voltage step

For the circuit

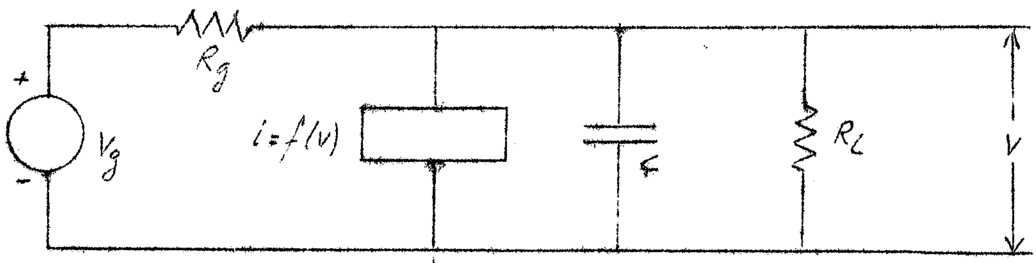

FIG. 5

one finds the equation

$$t = C \int_0^v \frac{dv}{\frac{v_g}{R_g} - f(v) - \frac{v}{R_p}}$$

where

$$R_p = \frac{R_L R_g}{R_L + R_g}$$

hence, with the notations employed in the preceding paragraph,

$$\tau_{s1} = \frac{2c}{\sqrt{q}}\left[tg^{-1}\frac{\frac{2I_p}{v_p^2}(v_2 - v_p) - \frac{1}{R_p}}{\sqrt{q}} - tg^{-1}\frac{2\frac{I_p}{v_p} + \frac{1}{R_p}}{-\sqrt{q}}\right]$$

$$\tau_{s2} = -\frac{2c}{\sqrt{-q}}\left[tgh^{-1}\frac{-2\frac{AI_p - I_v}{(v_x - v_v)^2}(v_f - v_v) - \frac{1}{R_p}}{\sqrt{-q}} - tgh^{-1}\frac{-2\frac{AI_p - I_v}{(v_x - v_v)} - \frac{1}{R_p}}{\sqrt{-q}}\right]$$

where $$q = \frac{4I_p}{v_p^2}\left(\frac{v_g}{R_g} - I_p - \frac{v_p}{R_p}\right) - \frac{1}{R_p^2}$$

As will be seen in par. 7 experimental results are in good agreement with these predictions.

The addition of series inductance L, leads to a differential equation of the following type

$$\frac{d^2v}{dt^2} + \left[\frac{1}{c}\frac{df}{dv} + \frac{R_g}{L}\right]\frac{dv}{dt} + \frac{R_g f(v) + v - v_g}{Lc} = 0$$

which is not soluble in an elementary fashion.

5 - Response to a voltage ramp.

For the circuit

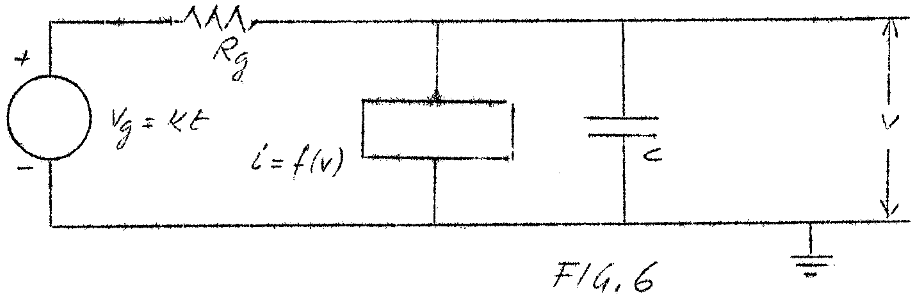

FIG. 6

the equation is

$$c\frac{dv}{dt} + f(v) = \frac{kt - v}{R_g}$$

whose solution is

$$v = v_0 + \frac{1}{2R_g k_1} - \frac{b''^{\frac{1}{3}}}{2az} - \frac{b''^{\frac{1}{3}}}{a}\sqrt{z}\;\frac{C_1 I'_{\frac{1}{3}} + I'_{-\frac{1}{3}}}{C_1 I_{\frac{1}{3}} + I_{-\frac{1}{3}}}$$

where

$$C_1 = \frac{I'_{-\frac{1}{3}}\left(\frac{2}{3}z_0^3\right) - \frac{M}{\sqrt{z_0}} I_{-\frac{1}{3}}\left(\frac{2}{3}z_0^3\right)}{\frac{M}{\sqrt{z_0}} I_{\frac{1}{3}}\left(\frac{2}{3}z_0^3\right) - I_{\frac{1}{3}}\left(\frac{2}{3}z_0^3\right)}$$

is the integration constant, determined by setting v=0 for t = 0. The slope of the output voltage waveform, i.e.

$$\frac{dv}{dt} = -\frac{1}{a}\left[\frac{b''^2}{(a''+b''t)^2} + \frac{b''}{(a''+b''t)}\left[\frac{C_1 I'_{\frac{1}{3}} + I'_{-\frac{1}{3}}}{C_1 I_{\frac{1}{3}} + I_{-\frac{1}{3}}}\right] + \right.$$
$$\left. + \frac{1}{2}(a''+b''t)\frac{d}{d\chi}\left(\frac{C_1 I'_{\frac{1}{3}} + I'_{-\frac{1}{3}}}{C_1 I_{\frac{1}{3}} + I_{-\frac{1}{3}}}\right)\right]$$

is only slightly dependent on K (the input voltage slope) for values of v close to v_x because the two first terms largely cancel each other. This verifies a well known experimental fact. In the above equations the following symbols have been used

$$b''^{\frac{2}{3}} z = a'' + b''t \; ; \qquad z_0 = \frac{a''}{b''^{\frac{2}{3}}}$$

$$a'' = \frac{K_1}{C}\left(\frac{v_0}{R_g C} + \frac{K_2}{C}\right) - \frac{1}{4R_g^2 C^2}$$

$$b'' = \frac{K_1}{C^2 R_g} K \; ; \qquad a = -\frac{K_1}{C} ; \qquad I_j = I_j\left(\frac{2}{3} z^{\frac{3}{2}}\right) \equiv I_j(\chi)$$

$$-M = \frac{1}{2z_0} + \frac{a'}{2b''^{1/3}} + \frac{a v_0}{b''^{1/3}}$$

$$\chi = \frac{2}{3}|z|^{\frac{3}{2}}$$

6 - General considerations.

Due to the negative resistance region of the TD's characteristic, it is quite possible for the device to oscillate when biased in this region. This fact poses a certain number of practical difficulties in designing suitable

FIGURE 8

INPUT–OUTPUT VOLTAGE CALCULATED CHARACTERISTIC FOR THE CIRCUIT

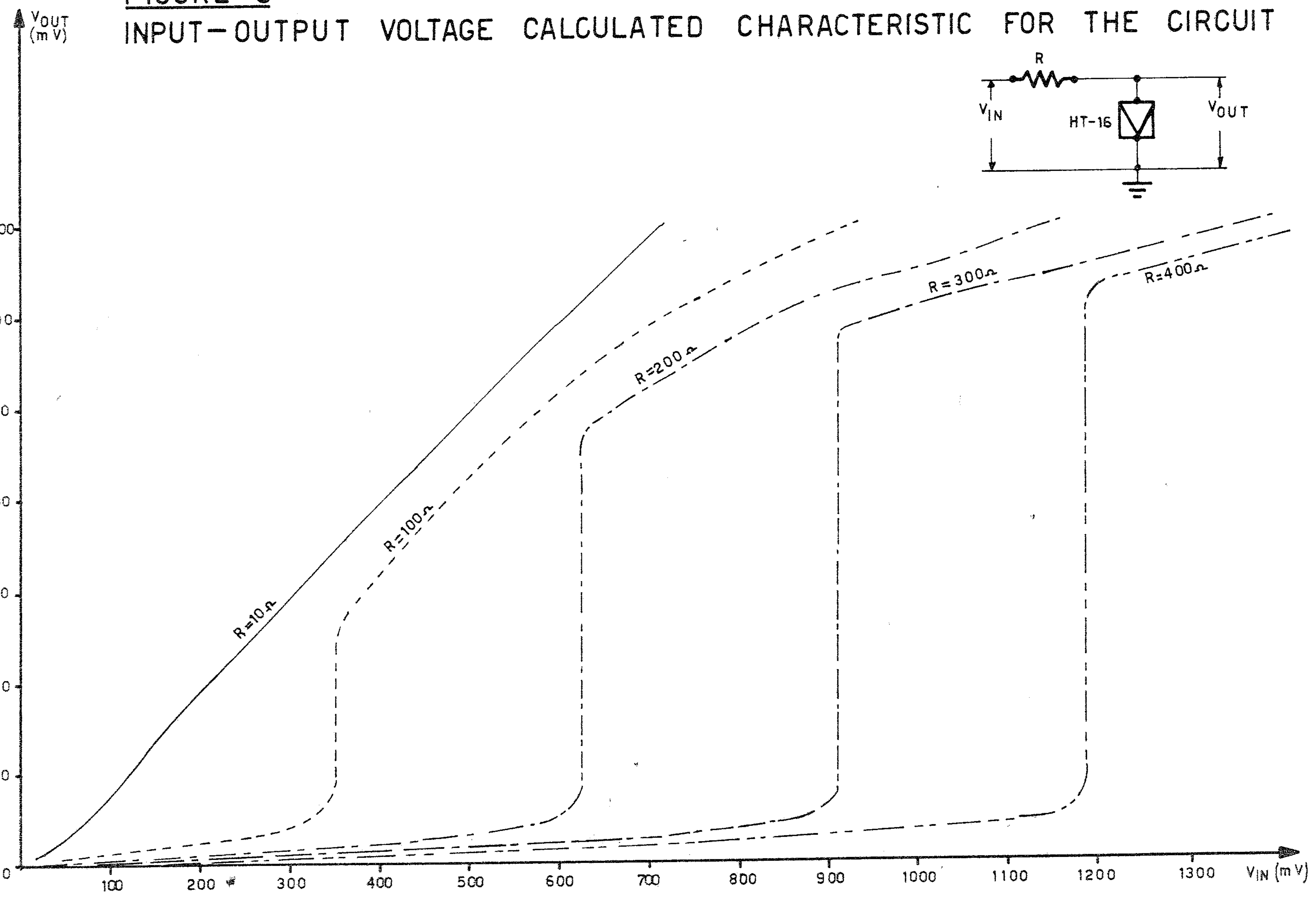

curve tracers to display the V-I curve. It has been shown[11] that for a negative resistance $-r$ to be stable when shunted by a positive resistance R the following inequalities must hold

$$\frac{L}{rC} < R < r$$

where L and C are total series inductance and shunt capacitance respectively. Since

$$r = \left| \frac{dV}{di} \right| = \frac{1}{\left| \frac{di}{dV} \right|}$$

is a function of voltage, the above relation must be verified for all r, i.e. for the minimum value that r may take over this range, i.e.

$$\frac{L}{r_{min} C} < R < r_{min}$$

where r_{min} is given by eq. (3).

Let us now consider the following circuit

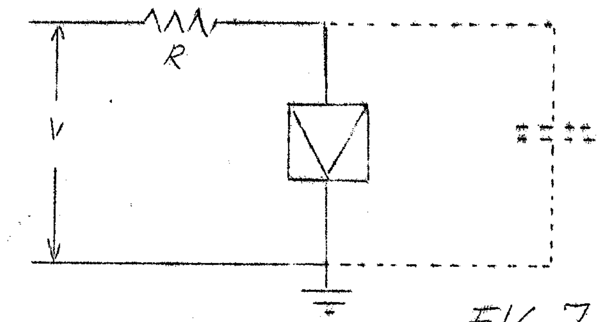

FIG. 7

For each value of V a load in the conventional manner can be drawn, and it is easily seen that the circuit will jump from a low to a high - voltage state (provided R is large enough) when

$$V \gtrsim V_p + R I_p$$

so that this simple circuit will act as a trigger or amplitude discriminator circuit. Input - output diagrams for a range of resistances are given in fig. 8. It is a well-known fact that loop gain-bandwidth is the major factor influencing speed and threshold dèfinition of trigger circuits[11-12]. Loop gain-bandwidth (GBW) products are easily calculated only assuming linearity: for non-linear circuits a comparison may be made by calculating GBW at maximum gain. For the tunnel - diode circuit above one obtains, again neglecting circuit inductance,

$$GBW \simeq \frac{g}{2\pi} \frac{1+R_g}{C} \text{ cycles/sec}$$

where $g = \frac{1}{r_{min}}$. For a 1 mA, 10 pF TD [13] one obtains,

$$GBW \simeq 1{,}2 \ 10^9 \text{ cycles/sec}$$

Whereas for a 50 mA, 25 pF TD[14] one obtains

$$GBW \simeq 24 \cdot 10^9 \text{ cycles/sec}$$

In contrast, for a vacuum tube trigger circuit using wide band pentodes (E 180F's) in a conventional arrangement, one finds

$$GBW \simeq 0{,}35 \ 10^9 \text{ cycles/sec}$$

The above figures clearly indicate the advantage of using tunnel diodes for such circuits.

7 - Fast discriminator coincidence circuit.

The block diagram of the fast discriminator - coincidence circuit is given in fig. 9. Input pulses greater than pre-set thresholds trigger the TD discriminators which in turn trigger the coincidence proper, which is therefore fed by standard pulses. Use of discriminators preceding the coincidence allows a large reduction in chance coincidences due to low-level background to be made. Circuit diagram is given in fig. 10.

Tunnel diode TD1 is current biased by d.c. emitter follower Q_1, diode D_1 being added to improve the discrimi

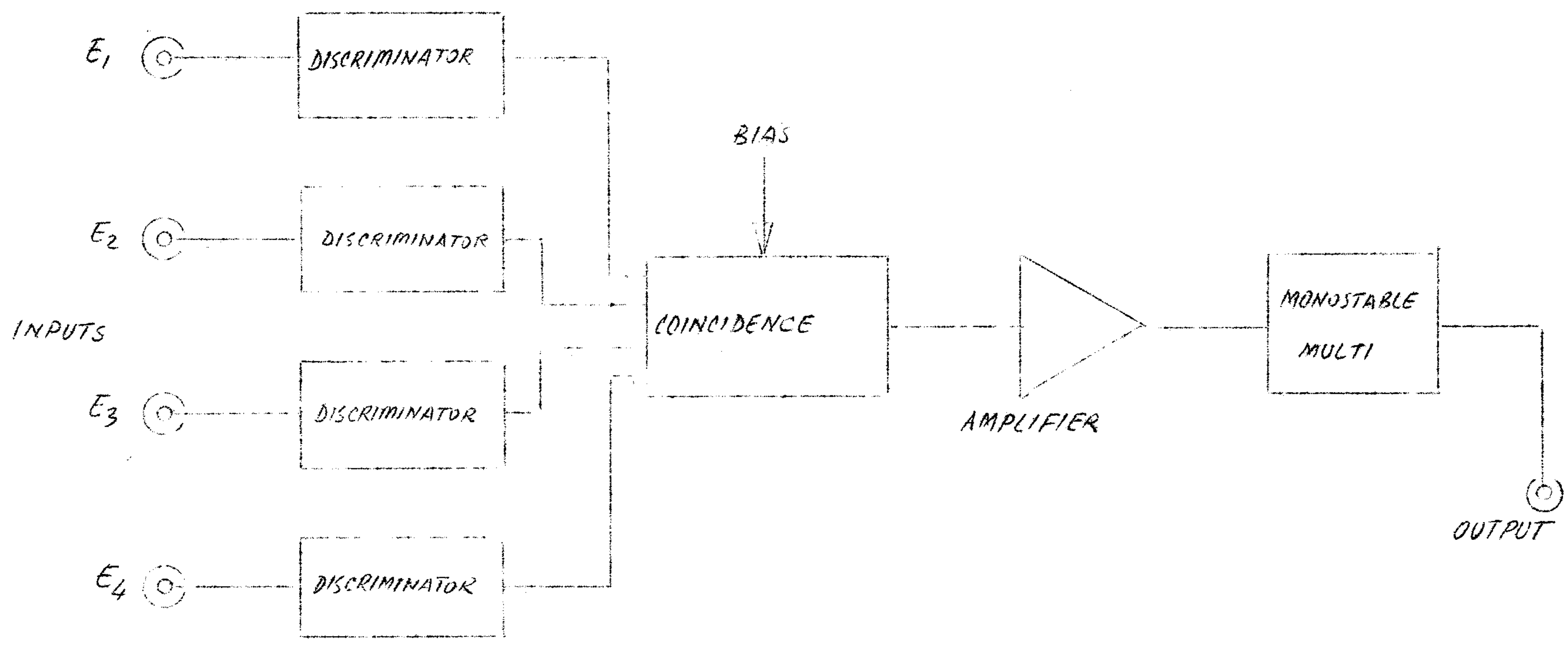

FIG. 9 - BLOCK DIAGRAM OF FAST COINCIDENCE

CIRCUIT DIAGRAM

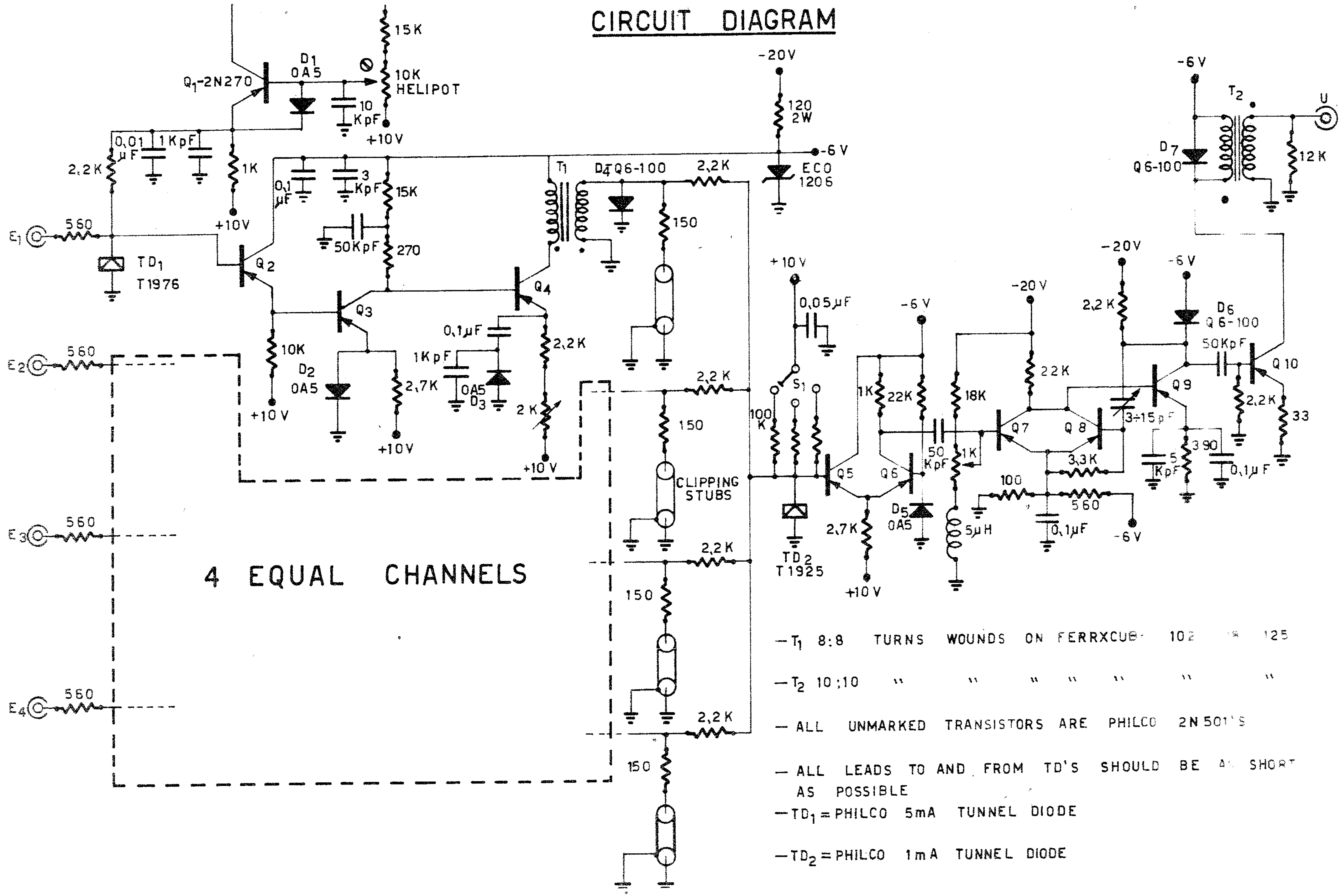

— T_1 8:8 TURNS WOUNDS ON FERRXCUBE 102 x 125

— T_2 10;10 " " " " " " "

— ALL UNMARKED TRANSISTORS ARE PHILCO 2N 501'S

— ALL LEADS TO AND FROM TD'S SHOULD BE AS SHORT AS POSSIBLE

— TD_1 = PHILCO 5mA TUNNEL DIODE

— TD_2 = PHILCO 1mA TUNNEL DIODE

nators linearity in the high ranges. Negative input pulses above the threshold trigger TD_1, are emitter-followed by Q_2 and turn Q_3 on. As Q_3 is normally off, this reduces pe destal and feed-through problems. Current drawn by transi stor Q_4 is almost entirely determined by its emitter resi stor and by the positive voltage supply. When Q_4 is turned off it therefore produces a standard pulse that is clipped by the subsequent shorting stub. Each discriminator therefore feeds a standard current pulse in TD_2; depending on the biasing conditions, the number of pulses necessary to trigger TD_2 may be 2,3 or 4. Selection is accomplished by rotating switch S_1, thereby changing order of coincidence. Anti-coincidence is accomplished simply by inverting the pulse produced by a discriminator, i.e. reversing one of the windings of pulse transformer T_1. When TD_2 triggers its (negative) output is amplified by long-tailed pair Q_5 and Q_6, thereby firing the monostable circuit composed of Q_7, Q_8 and Q_9(16). Q_{10} is added for impedance matching. Out put is 5 volts - positive or negative - into 125 ohms, 50 ns duration. As the input impedance of the circuit is not well-defined, it is imperative that connecting cables be cor rectly matched at the photomultiplier end. The discrimina tor calibration curve is shown in fig. 11, while the delay time jitter (for long pulses) is shown in fig. 12 and agre es well with theoretical predictions based on the foregoing theory. Delay time jitter for short (20 nsec) pulses is much less, about 5 nsec for a pulse whose amplitude is 1% above threshold. The discriminator's dead time is of the order of 50 nsec and it will trigger up to about 20 Mc. Coincidence resolving time is quite good: the accompanying fig. 13 shows a full width at half maximum of 4 nsec. The curve was taken using cosmic rays detected by two 28x10x1cm plastic scintillators viewed by RCA 6810A photomultipliers

FIG. 11

DISCRIMINATOR CALIBRATION CURVE

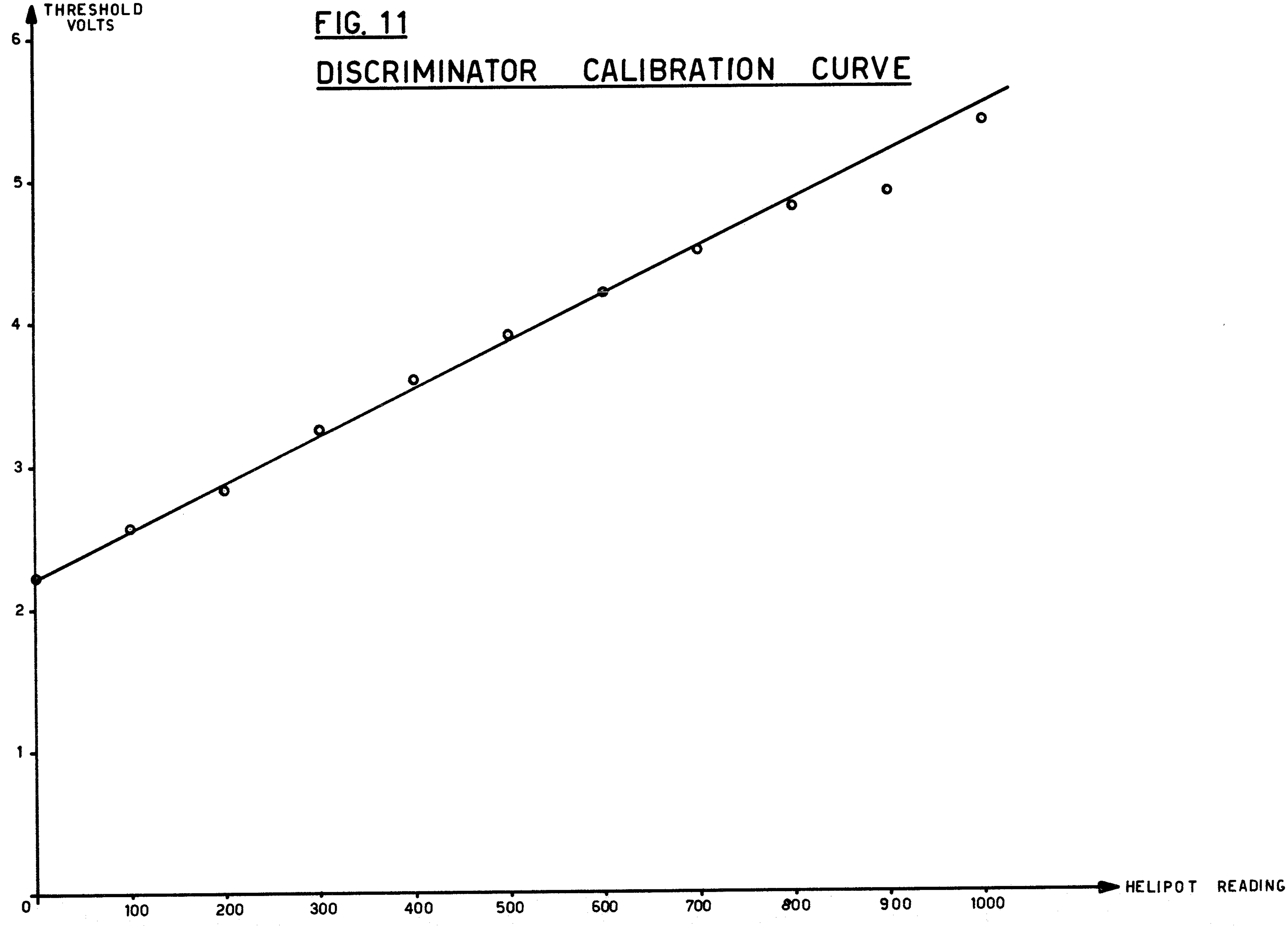

FIGURE 12

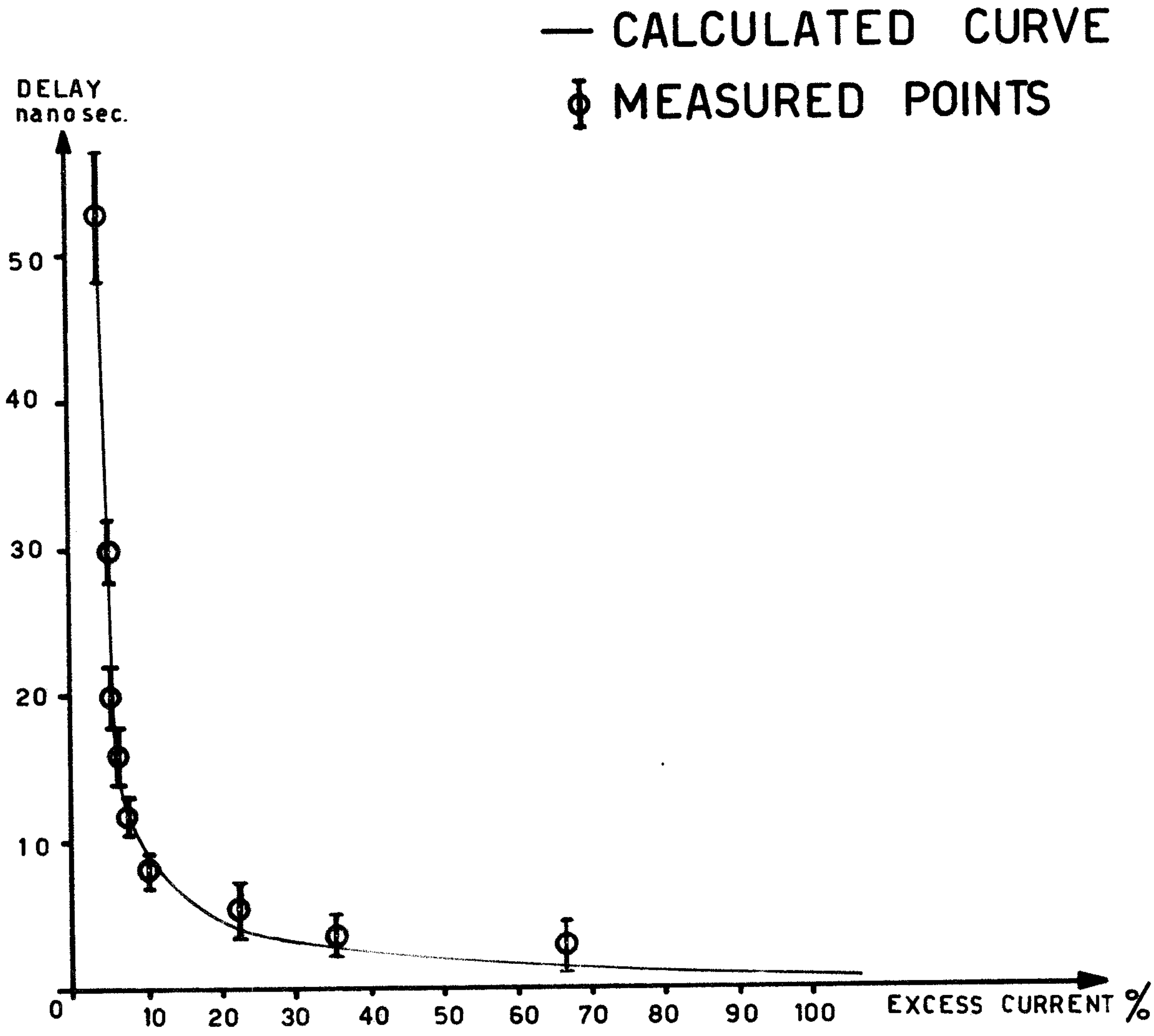
— CALCULATED CURVE
MEASURED POINTS
DELAY
nano sec.
50
40
30
20
10
0
10
20
30
40
50
60
70
80
90
100
EXCESS CURRENT %

FIG. 13

COINCIDENCE RESOLUTION CURVE

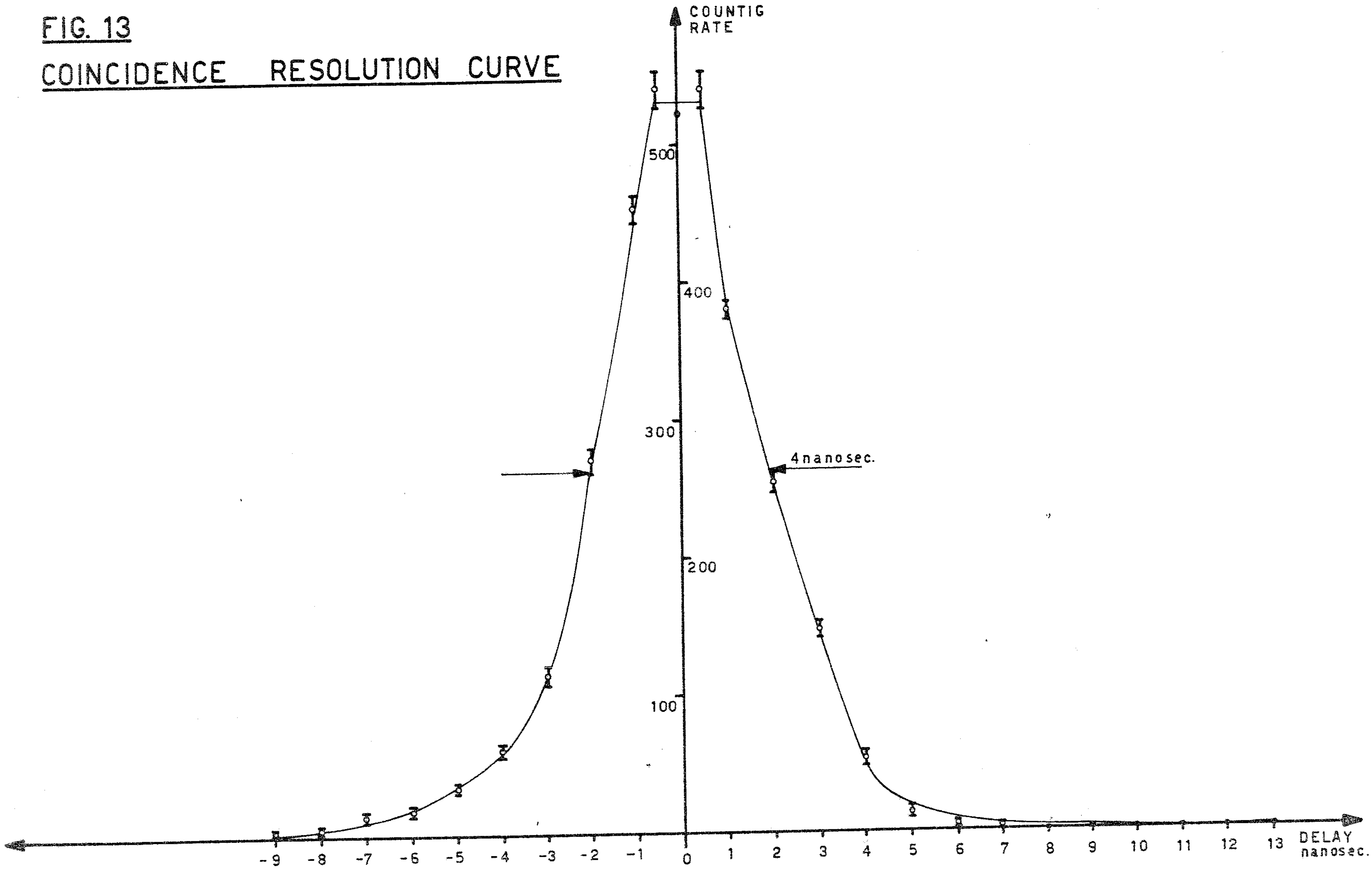

and is therefore almost entirely due to the photostatistics. Clipping stubs were 5 nsec long.

Acknowledgements.

The Authors wish to express their thanks to Prof. I.F. Quercia for constant encouragement and advice and to Messrs. C. Dardini and R. Rizzi who were of great help in setting up, and testing the circuitry.

Notes

(1) L. Esaki: Phys. Rev. 109, 603, 1958
(2) H.S. Sommers: Proc. IRE, 47, 1201, 1959
(3) K.K.N. Chase: Proc. I.R.E. 47, 1268, 1959
(4) P. Spiegel: Rev. Sci. Instr. 31, 754, 1960
(5) E. Goto et al.: IRE Trans. EC-9, 25, 1960
(6) J. Rajchmann, RCA Labs: Private Communication.
(7) W.F. Chow: IRE Trans. EC-9, 295, 1960
(8) R.H. Bergman: IRE Trans. EC-9, 430, 1960
(9) Variations of Capacitance with voltage are neglected
(10) See e.g. J. Mey Rev. Sci. Instr.: 30, 282, 1959.
(11) U.S. Davidsohn et al. Electronic Design, Feb. 3, 1960
(12) M. Brown: Rev. Sci. Instr. 30, 169, 1959
(13) C.Infante: Nucl. Instr. and Meth. 9, 102, 1960
(14) T 1975 made by Philco Corp.
(15) IN3130 made by Radio Corp. of America.
(16) R.H. Miller: Rev. Sci. Instr. 30, 395, 1959